





# Wall-induced translation of a rotating particle in a shear-thinning fluid

Ye Chen<sup>1,2</sup>,‡, Ebru Demir<sup>1</sup>,‡, Wei Gao<sup>3</sup>, Y.-N. Young<sup>2</sup> and On Shun Pak<sup>1</sup>,†

(Received 14 July 2021; revised 21 August 2021; accepted 28 August 2021)

Particle—wall interactions have broad biological and technological applications. In particular, some artificial microswimmers capitalize on their translation—rotation coupling near a wall to generate directed propulsion. Emerging biomedical applications of these microswimmers in complex biological fluids prompt questions on the impact of non-Newtonian rheology on their propulsion. In this work, we report some intriguing effects of shear-thinning rheology, a ubiquitous non-Newtonian behaviour of biological fluids, on the translation—rotation coupling of a particle near a wall. One particularly interesting feature revealed here is that the wall-induced translation by rotation can occur in a direction opposite to what might be intuitively expected for an object rolling on a solid substrate. We elucidate the underlying physical mechanism and discuss its implications on the design of micromachines and bacterial motion near walls in complex fluids.

Key words: micro-organism dynamics

## 1. Introduction

The motion of microparticles near boundaries is of broad interest because the proximity of boundaries is all but unavoidable in most real situations. Particle—wall interactions can have important biological and technological implications such as the segregation of blood cells and platelets in vessels and the techniques of particle manipulation in microfluidic channels. More recently, the locomotion of bacteria near surfaces and its connection to biofilm formation have received considerable attention (Lauga *et al.* 2006; Lemelle *et al.* 2010; Di Leonardo *et al.* 2011; Morse *et al.* 2013). In the development of artificial microswimmers, it is also crucial to account for the presence of boundaries, which may

† Email address for correspondence: opak@scu.edu ‡ These authors contribute equally to this work.

<sup>&</sup>lt;sup>1</sup>Department of Mechanical Engineering, Santa Clara University, Santa Clara, CA 95053, USA

<sup>&</sup>lt;sup>2</sup>Department of Mathematical Sciences, New Jersey Institute of Technology, Newark, NJ 07102, USA

<sup>&</sup>lt;sup>3</sup> Andrew and Peggy Cherng Department of Medical Engineering, California Institute of Technology, Pasadena, CA 91125, USA

lead to propulsion enhancement or hindrance, and trapping or guiding of these swimmers (Spagnolie & Lauga 2012; Takagi *et al.* 2014; Elgeti & Gompper 2016). In particular, a class of artificial microswimmers, known as surface walkers or microrollers, exploit their interactions with nearby surfaces to generate directed propulsion (Tierno *et al.* 2008; Sing *et al.* 2010; Driscoll *et al.* 2017). These microswimmers are driven into rotation typically by external magnetic fields. Symmetry breaking in the proximity of a boundary rectifies their rotation into translation, analogous to rolling of a wheel on a solid surface. The simplicity and effectiveness of these microrollers demonstrate vast opportunities for applications in targeted therapeutics and microsurgery (Alapan *et al.* 2020; Ahmed *et al.* 2021).

Particle—wall interactions at low Reynolds numbers are well studied in a Newtonian fluid. Emerging biomedical applications of micromachines in complex biological fluids, however, prompt new questions on the impact of non-Newtonian rheology on these interactions (Elfring & Lauga 2015; Sznitman & Arratia 2015). In particular, biological fluids such as blood and mucus are typically shear-thinning fluids (Cho & Kensey 1991; Gijsen, van de Vosse & Janssen 1999; Li et al. 2008), which lose viscosity with applied strain rates due to changes in the fluid microstructure. Recent studies have uncovered the profound effects of shear-thinning rheology on locomotion (Montenegro-Johnson, Smith & Loghin 2013; Vélez-Cordero & Lauga 2013; Datt et al. 2015; Li & Ardekani 2015; Montenegro-Johnson 2017), impacting both living micro-organisms and artificial swimmers (Gagnon, Keim & Arratia 2014; Gagnon & Arratia 2016; Park et al. 2016; Gómez et al. 2017; Demir et al. 2020; Qu & Breuer 2020). The non-Newtonian fluid behaviour also enables locomotion otherwise impossible in a Newtonian fluid (Qiu et al. 2014; Han et al. 2020).

In this work, we report some intriguing effects of shear-thinning rheology on the translation–rotation coupling of a particle near a wall. Such coupling is relevant to not only the propulsion of microrollers but also the near-wall dynamics of swimming bacteria in complex fluids. One particularly interesting feature revealed in this work is that the wall-induced translation by a rotating particle can occur in a direction opposite to what might be intuitively expected in a Newtonian fluid. We elucidate the physical mechanism underlying the counterintuitive phenomena and discuss its implications on the design and control of micromachines in complex biological fluids. Our results also suggest a plausible mechanism for the observed directional change in circular motion of swimming bacteria near a solid wall in complex fluids. In addition, the features reported may inspire novel techniques for particle manipulation in microfluidics with non-Newtonian flows and microrheological measurements.

## 2. Theoretical framework

Classical results of wall-induced translation of a rotating object were obtained in a Newtonian fluid in the Stokes regime. For the three-dimensional (3-D) Stokes flow around a rotating sphere near a plane wall (Dean & O'Neill 1963; O'Neill 1964, 1967), the sphere translates parallel to the wall in a direction consistent with the rolling of a sphere along the wall, without any velocity component normal to the wall,  $U = Ue_x$ ; see notation and set-up in figure 1. The direction of induced translation can be understood as a consequence of the fact that the rotating sphere causes higher velocity gradients in the fluid gap between the sphere and the wall and hence a larger hydrodynamic force on the side of the sphere closer to the wall than that on the other side. The force imbalance thus drives the sphere to translate in a direction expected for a rolling sphere on a solid substrate via friction asymmetry.

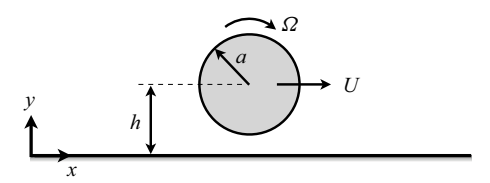


Figure 1. Wall-induced translation of a rotating cylinder or sphere of radius a at a distance h above a plane wall. Upon a prescribed rotational velocity  $\Omega = -\Omega e_z$ , the particle translates parallel to the wall with an unknown velocity  $U = Ue_x$ . In this work, the case U > 0 (U < 0) is referred to as the forward (backward) mode.

Surprisingly, a later two-dimensional (2-D) analysis by Jeffrey & Onishi (1981) found that the 2-D Stokes flow around a rotating cylinder near the wall yields exactly zero induced translation, despite the broken symmetry due to the wall. Here, we revisit these classical results on translation–rotation coupling near a wall and examine how shear-thinning rheology modifies the coupling in both the 2-D and 3-D cases. In particular, the fact that there is no induced translation in the Newtonian 2-D case allows us to attribute any translation in a shear-thinning fluid in two dimensions solely to the non-Newtonian rheology.

## 2.1. Asymptotic analysis

We begin our analysis with the momentum and continuity equations for an incompressible flow in the low-Reynolds-number limit,

$$\nabla \cdot \boldsymbol{\sigma} = \mathbf{0}, \quad \nabla \cdot \boldsymbol{u} = 0, \tag{2.1a,b}$$

where u is the fluid velocity,  $\sigma = -pI + \tau$  is the stress tensor, and p and  $\tau$  are the pressure and the deviatoric stress, respectively. To capture the shear-thinning behaviour, we use the Carreau constitutive equation, which was shown to describe effectively the viscosity  $\eta$  of different biological fluids (Bird, Armstrong & Hassager 1987; Vélez-Cordero & Lauga 2013),

$$\eta = \eta_{\infty} + (\eta_0 - \eta_{\infty})(1 + \lambda^2 |\dot{\gamma}|^2)^{(n-1)/2}.$$
 (2.2)

Here  $\eta_0$  and  $\eta_\infty$  represent, respectively, the zero- and infinite-shear-rate viscosities, and the strain-rate tensor  $\dot{\gamma} = \nabla u + (\nabla u)^T$  has a magnitude  $|\dot{\gamma}| = (\dot{\gamma}_{ij}\dot{\gamma}_{ij}/2)^{1/2}$ . The power-law index n < 1 characterizes the degree of shear thinning, and  $1/\lambda$  characterizes the critical shear rate at which the non-Newtonian behaviour becomes significant. Henceforth, we use dimensionless variables with time, length and stress scaled by  $1/\Omega$ , a and  $\eta_0\Omega$ , respectively. The dimensionless nonlinear constitutive equation is therefore given by

$$\tau = [\beta + (1 - \beta)(1 + Cu^2|\dot{\gamma}|^2)^{(n-1)/2}]\dot{\gamma}, \tag{2.3}$$

where the Carreau number,  $Cu = \lambda \Omega$ , compares the rotational rate to the critical shear rate of the shear-thinning fluid, and  $\beta = \eta_{\infty}/\eta_0 \le 1$  is the viscosity ratio.

We consider the weakly nonlinear (non-Newtonian) limit by expanding

$$\{u, \dot{\gamma}, p, \sigma, U\} = \{u_0, \dot{\gamma}_0, p_0, \sigma_0, U_0\} + \epsilon\{u_1, \dot{\gamma}_1, p_1, \sigma_1, U_1\} + O(\epsilon^2), \tag{2.4}$$

where  $\epsilon = 1 - \beta \ll 1$ . The zeroth-order solution corresponds to the Newtonian flow, satisfying  $\nabla \cdot \boldsymbol{\sigma}_0 = \mathbf{0}$  and  $\nabla \cdot \boldsymbol{u}_0 = 0$ , where  $\boldsymbol{\sigma}_0 = -p_0 I + \dot{\boldsymbol{\gamma}}_0$  is the Newtonian

fluid stress. At  $O(\epsilon)$ , the momentum and continuity equations are given by

$$\nabla \cdot \boldsymbol{\sigma}_1 = \mathbf{0}, \quad \nabla \cdot \boldsymbol{u}_1 = 0, \tag{2.5a,b}$$

where the first non-Newtonian correction to the fluid stress reads

$$\sigma_1 = -p_1 l + \dot{\boldsymbol{\gamma}}_1 + \boldsymbol{A} \tag{2.6}$$

and

$$\mathbf{A} = [-1 + (1 + Cu^2 |\dot{\gamma}_0|^2)^{(n-1)/2}]\dot{\mathbf{\gamma}}_0. \tag{2.7}$$

The goal here is to obtain the first non-Newtonian correction to the induced translational velocity  $U_1$ . We utilize the Lorentz reciprocal theorem (Lauga 2014; Elfring 2017; Masoud & Stone 2019) to calculate the velocity  $U_1$ , bypassing calculations of the velocity and pressure fields at  $O(\epsilon)$ . As a remark, the reciprocal theorem is particularly useful for determining quantities such as the velocity of a particle and the force and torque on a particle. However, this integral approach does not provide detailed information such as the distribution of viscosity and the distribution of surface traction on a particle, which require calculations of the pressure and velocity fields.

## 2.2. The reciprocal theorem

To apply the reciprocal theorem, we consider an auxiliary Stokes flow problem, whose flow field  $(\hat{u})$  and fluid stress  $(\hat{\sigma})$  satisfy

$$\nabla \cdot \hat{\boldsymbol{\sigma}} = \mathbf{0}, \quad \nabla \cdot \hat{\boldsymbol{u}} = 0, \tag{2.8a,b}$$

where

$$\hat{\boldsymbol{\sigma}} = -\hat{p}\boldsymbol{I} + \hat{\dot{\boldsymbol{\gamma}}},\tag{2.9}$$

and  $\hat{p}$  and  $\hat{\dot{\gamma}} = \nabla \hat{u} + (\nabla \hat{u})^{T}$  denote, respectively, the pressure and the strain-rate tensor in the auxiliary flow problem.

Taking the inner product of the momentum equation in (2.5a) with  $\hat{u}$  and the inner product of the momentum equation in (2.8a) with  $u_1$ , we obtain the relation

$$\hat{\boldsymbol{u}} \cdot \nabla \cdot \boldsymbol{\sigma}_1 = \boldsymbol{u}_1 \cdot \nabla \cdot \hat{\boldsymbol{\sigma}}. \tag{2.10}$$

We then integrate (2.10) over the fluid volume V and employ the divergence theorem to obtain

$$\int_{\mathcal{S}} \boldsymbol{n} \cdot \hat{\boldsymbol{\sigma}} \cdot \boldsymbol{u}_1 \, d\mathcal{S} - \int_{\mathcal{S}} \boldsymbol{n} \cdot \boldsymbol{\sigma}_1 \cdot \hat{\boldsymbol{u}} \, d\mathcal{S} = \int_{\mathcal{V}} \boldsymbol{\sigma}_1 : \nabla \hat{\boldsymbol{u}} \, d\mathcal{V} - \int_{\mathcal{V}} \hat{\boldsymbol{\sigma}} : \nabla \boldsymbol{u}_1 \, d\mathcal{V}, \quad (2.11)$$

where n is the unit normal vector on surface S.

By substituting the fluid stress in the first-order problem given by (2.6) and that in the auxiliary flow problem given by (2.9) into the integrands on the right-hand side of (2.11), one can show that  $\sigma_1: \nabla \hat{u} - \hat{\sigma}: \nabla u_1 = \mathbf{A}: \nabla \hat{u}$  due to the continuity equations ( $\nabla \cdot \hat{u} = \nabla \cdot u_1 = 0$ ) and symmetry ( $\dot{\gamma}_1: \nabla \hat{u} = \hat{\gamma}: \nabla u_1$ ). Moreover, suppose the particle in the auxiliary problem translates with velocity  $\hat{U}$  without rotation, the integral relation (2.11) then becomes

$$\hat{F} \cdot U_1 - F_1 \cdot \hat{U} = \int_{\mathcal{V}} \mathbf{A} : \nabla \hat{\mathbf{u}} \, d\mathcal{V}, \tag{2.12}$$

where  $\hat{F} = \int_{\mathcal{S}} \mathbf{n} \cdot \hat{\sigma} \, d\mathcal{S}$  and  $F_1 = \int_{\mathcal{S}} \mathbf{n} \cdot \sigma_1 \, d\mathcal{S}$  denote, respectively, the force on the particle in the auxiliary and first-order problems. By enforcing the force-free condition

 $(F_1 = \int_{\mathcal{S}} \mathbf{n} \cdot \mathbf{\sigma}_1 \, \mathrm{d}\mathcal{S} = \mathbf{0})$ , one obtains the non-Newtonian correction to the induced translational velocity from the reciprocal theorem as

$$\hat{F} \cdot U_1 = \int_{\mathcal{V}} \mathbf{A} : \nabla \hat{\mathbf{u}} \, \mathrm{d} \mathcal{V}. \tag{2.13}$$

Here, only known Newtonian solutions in the zeroth-order  $(u_0)$  and auxiliary flow  $(\hat{u})$  problems are required to determine the non-Newtonian correction to the speed,  $U_1$ . We apply this integral theorem in 2-D and 3-D set-ups and discuss the results in §§ 3.1 and 3.2, respectively.

## 2.3. Numerical solution

To compare with the results from the asymptotic analysis, we also performed full numerical simulations of the momentum and continuity equations (2.1a,b) together with the Carreau constitutive equation (2.3) using the finite element method implemented in the COMSOL Multiphysics environment. A 2-D rectangular computational domain of size  $1000a \times 500a$  (in the x- and y-directions, respectively) is used to simulate the dynamics of a rotating cylinder near a wall. For a rotating sphere near a wall, we take advantage of the symmetry about the x-y plane through the centre of the sphere and use a 3-D computational domain consisting of a rectangular prism of size  $250a \times (125a + h) \times 125a$  (in the x-, y- and z-directions, respectively) to simulate only half of the full domain. A known angular velocity together with the unknown translational velocity are prescribed on the particle surface as the boundary condition.

The momentum and continuity equations are solved simultaneously with the force-free condition to determine the induced translational velocity in different directions. Here, P2+P1 (second order for fluid velocity and first order for pressure) triangular/tetrahedral mesh elements are used for the 2-D/3-D simulations, with local mesh refinement near the rotating cylinder/sphere. The degree of freedom is of the order of  $(1.2-2) \times 10^6$  for the 2-D simulations and  $(3.5-6) \times 10^6$  for the 3-D simulations, depending on the distance of the cylinder/sphere from the wall. We use the Multifrontal Massively Parallel Sparse (MUMPS) direct solver for all simulations. In addition to comparing with the results from the asymptotic analysis, we validated the numerical implementation against analytical solutions in a Newtonian fluid in previous works (Dean & O'Neill 1963; O'Neill 1964, 1967; Jeffrey & Onishi 1981).

## 3. Results and discussion

# 3.1. Two-dimensional problem

First, we revisit the surprising result that a rotating cylinder does not translate near a wall in the Stokes limit (Jeffrey & Onishi 1981),  $U_0 = \mathbf{0}$ , and calculate the leading-order translational velocity,  $\epsilon U_1$ , induced by shear-thinning rheology. We employ the result from the integral theorem (2.13) with two known exact Newtonian solutions by Jeffrey & Onishi (1981): the Stokes flow around a cylinder rotating near a plane wall,  $u_0$ , and the Stokes flow around a cylinder translating parallel to wall in the auxiliary problem,  $\hat{u}$ . Substituting these flows into (2.13) and evaluating the integral numerically, we obtain the leading-order translational velocity parallel to the wall,  $U = Ue_x \sim \epsilon U_1 e_x$ , as shown in figure 2(a). The asymptotic results (lines) agree well with results by numerical simulations (symbols) at different relative heights above the wall. Figure 2(b) compares the asymptotic

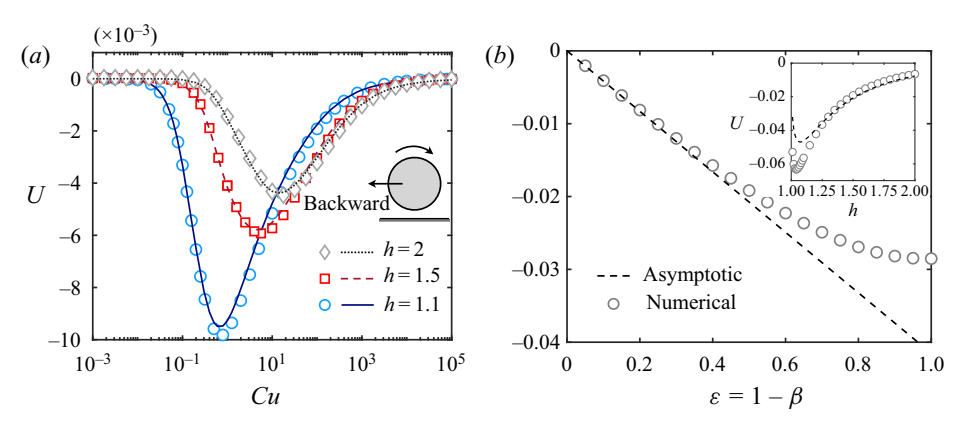


Figure 2. Wall-induced translation of a rotating cylinder in a shear-thinning fluid. (a) The induced translational velocity U (scaled by  $a\Omega$ ) as a function of the Carreau number Cu for different distances h (scaled by a) from the wall. Asymptotic results via the reciprocal theorem (lines) agree well with results by full numerical simulations (symbols). The induced translation occurs in the backward mode (U < 0) in a shear-thinning fluid, opposite to what might be intuitively expected for an object rolling on a solid substrate. Here,  $\beta = 0.9$  and n = 0.25. (b) The translational velocity U as a function of  $\epsilon = 1 - \beta$  with a distance h = 1.5 from the wall. Inset: U as a function of h with a viscosity ratio h = 0.5. Here, h = 0.25 and h = 1.

and numerical results for a full range of  $\epsilon = 1 - \beta$ ; the asymptotic result is still effective in capturing the qualitative behaviour with an intermediate value of  $\beta$  (inset).

From these results, first, unlike the Newtonian case, the shear-thinning rheology gives rise to a parallel (to the wall) translation of a rotating cylinder. Second, similar to the Newtonian case, numerical simulations found negligibly small induced translation normal to the wall, consistent with the asymptotic result via the reciprocal theorem using the Stokes flow around a cylinder translating normal to the wall (Jeffrey & Onishi 1981) as the auxiliary problem. The absence of induced translation normal to the wall in a shear-thinning fluid is in contrast to the scenarios where other types of nonlinearities such as fluid elasticity, wall elasticity and inertial effects are present (Leal 1980; Wang & Joseph 2003; Daddi-Moussa-Ider *et al.* 2018*b*; Fang *et al.* 2020). Third, our results reveal an interesting feature that the induced translation occurs in the negative *x*-direction (referred to as the backward mode in this work), opposite to what might be intuitively expected for an object rolling along a solid surface.

To develop some understanding of these results, we examine the viscosity distribution around the rotating cylinder, when it is not free to translate. Under this set-up we analyse the hydrodynamic force on the rotating cylinder and probe any resulting force imbalance that drives a translation. As a reference, in an unbounded domain, the rotational motion of the cylinder reduces the fluid viscosity symmetrically around the cylinder (figure 3(a), top panel). The presence of the wall breaks the up-down symmetry and causes higher velocity gradients in the fluid gap below the cylinder than in the fluid above it. When the fluid is shear-thinning, although the viscosity around the cylinder decreases generally, the viscosity in the fluid gap is reduced to a greater extent due to higher velocity gradients, as shown in the bottom panel of figure 3(a). The less viscous fluid below the cylinder therefore leads to a weaker hydrodynamic force on the lower half of the cylinder ( $F_{\ell}$ ; acting to the right) compared with the force on the upper half ( $F_u$ ; acting to the left), as shown in figure 3(b) for different Cu. The force imbalance ( $F_{\ell} < F_u$ ; net force acting to the left) thus drives the rotating cylinder to translate to the left in the backward mode.

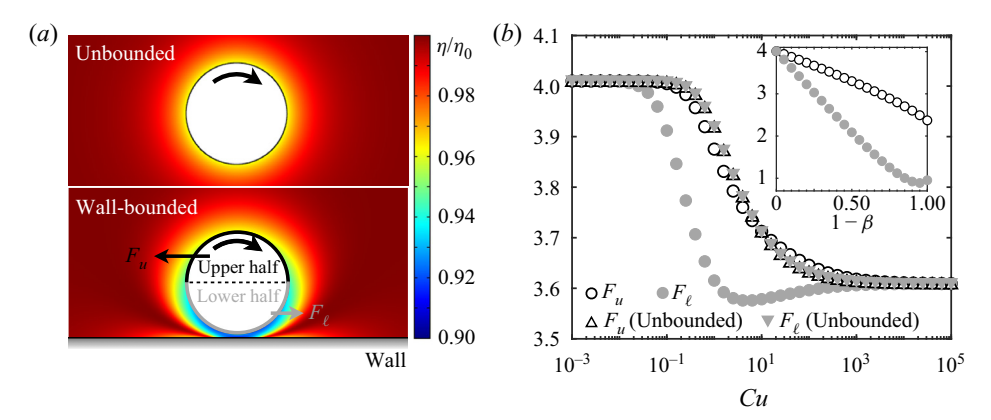


Figure 3. (a) Viscosity map  $(\eta/\eta_0)$  around a rotating cylinder in an unbounded (top panel) and wall-bounded (bottom panel) domains, when the cylinder is not free to translate. In an unbounded domain, the hydrodynamic force on the upper (open triangles,  $F_u$ ) and lower (filled triangles,  $F_\ell$ ) half of the cylinder are equal in magnitude in a shear-thinning fluid as shown in (b). The combined effect of shear-thinning viscosity and symmetry breaking by the wall induces a weaker hydrodynamic force on the lower half of the cylinder (filled circles) than that on the upper half (open circles) for different values of Cu. The viscosity maps shown in (a) correspond to the case Cu=0.8, around which the maximum translational speed occurs for a rotating cylinder at a distance h=1.1 from the wall. In (b), forces are scaled by  $\eta_0 a^2 \Omega$ . The force imbalance on the cylinder drives it to translate in the backward mode. Inset: the force on the upper (open circles) and lower (filled circles) half of the cylinder as a function of  $1-\beta$ . Here, in both panels,  $\beta=0.9$  (except for the inset) and n=0.25.

We note that the broken spatial symmetry due to the wall alone is insufficient to generate the asymmetric forces in a Newtonian fluid ( $F_\ell = F_u$  when Cu = 0). The emergence of induced translation in two dimensions thus requires the combined presence of shear-thinning effect and spatial symmetry breaking. At an exceedingly large Cu, the fluid is largely shear-thinned and the rotating cylinder is surrounded by a virtually Newtonian fluid with the infinite-shear-rate viscosity,  $\eta_\infty$ ; the asymmetry in force therefore decays, inducing vanishingly small translation when  $Cu \gg 1$ .

# 3.2. Three-dimensional problem

In contrast to the 2-D case, in three dimensions a rotating sphere translates parallel to the wall even in a Newtonian fluid,  $U_0 = U_0 e_x$  with  $U_0 > 0$ , in a direction consistent with the rolling of a sphere along the wall (the forward mode). The Newtonian translational velocity can be obtained based on analytical results obtained by O'Neill (1964, 1967) and Dean & O'Neill (1963). Here, we determine how shear-thinning rheology impacts the wall-induced translation of a rotating sphere.

Similar to the 2-D analysis, we obtain the non-Newtonian correction  $U_1 = U_1 e_x$  via the reciprocal theorem (2.13) but with two different Newtonian solutions: we use the Stokes flows around a sphere rotating (Dean & O'Neill 1963) and translating (O'Neill 1964, 1967) near a plane wall, respectively, for  $u_0$  and  $\hat{u}$  in (2.13). In figure 4(a), the results from the asymptotic analysis (lines) and numerical simulations (symbols) agree well in the weakly non-Newtonian regime with a viscosity ratio  $\beta = 0.9$ . The induced translation still occurs in the forward mode for varying Cu. The shear-thinning effect, which drives a rotating cylinder to translate in the backward mode, acts only to reduce the translational speed of a rotating sphere in the forward mode in this weakly nonlinear regime. We attribute the speed reduction observed here to the same physical mechanism explained in the 2-D case: compared with the Newtonian velocity ( $U_0 > 0$ ), the non-Newtonian

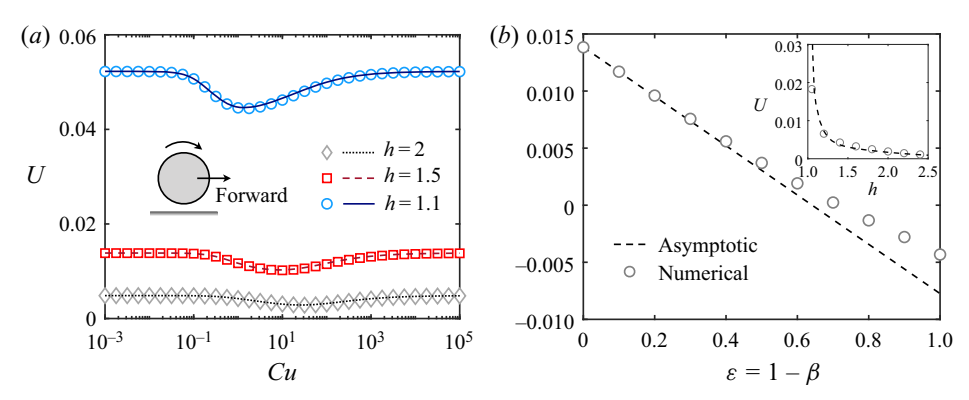


Figure 4. Wall-induced translation of a rotating sphere in a shear-thinning fluid. (a) The induced translational velocity U (scaled by  $a\Omega$ ) as a function of Cu for different distances h (scaled by a) from the wall. The rotating sphere translates in the forward mode (U>0) in this weakly non-Newtonian regime with a viscosity ratio  $\beta=0.9$ . Here, n=0.25. (b) The translational velocity U as a function of  $\epsilon=1-\beta$  with a distance h=1.5 from the wall. Asymptotic and numerical results agree well when  $\epsilon$  is relatively small. Inset: U as a function of h with a viscosity ratio  $\beta=0.5$ . Here, n=0.25 and Cu=1.

contribution acts in the opposite direction ( $\epsilon U_1 < 0$ ) but with a smaller magnitude in this weakly non-Newtonian regime ( $\epsilon \ll 1$ ), causing only a speed reduction without directional change. This leads to the hypothesis that a sufficiently strong shear-thinning effect could offset the Newtonian speed and ultimately drive the rotating sphere to translate in the backward mode similar to the 2-D case. Both asymptotic and numerical results in figure 4(b) show that backward translation can indeed occur for larger values of  $\epsilon$ .

We use numerical simulations to further probe the behaviour beyond the weakly non-Newtonian regime in figure 5. As shown in figure 5(a), when the shear-thinning effect is more substantial ( $\beta=0.1$ ), the rotating sphere can switch from translating in the forward mode to the backward mode beyond a critical value of Cu, depending on the height h above the wall. It is also noteworthy that the maximum backward speed occurring at the optimal Cu can be comparable to (e.g. when h=1.1) or even greater than the forward speed in the Newtonian limit (e.g. when h=1.5 and h=2). When Cu becomes exceedingly large, the Newtonian behaviour is recovered and the rotating sphere returns to translate in the forward mode. Figure 5(b) indicates the direction of induced translation for different values of Cu and  $\beta$ . We remark that, similar to the 2-D case, there is no translation normal to the wall in both Newtonian and shear-thinning fluids.

Based on our results, we provide an estimate of the magnitude of translational speed induced by this new mechanism in a typical experimental set-up with microrollers (Driscoll *et al.* 2017). Consider a spherical microroller of radius  $a=0.66~\mu m$  rotating with  $\Omega=100~{\rm s}^{-1}$  at a height  $h=1.0~\mu m$  above the wall. With a relative height of  $h/a\approx 1.5$ , from figure 5(a) we estimate a Newtonian (Cu=0) forward translational speed,  $U/a\Omega\approx 0.014$  or  $U\approx 1~\mu m~{\rm s}^{-1}$ , consistent with the order of magnitude in previous measurements in a Newtonian fluid (Driscoll *et al.* 2017). The corresponding speed in a shear-thinning fluid depends on specific fluid properties. The shear-thinning time scale  $\lambda$  of biological fluids can range from a tenth of a second to seconds for blood (Cho & Kensey 1991; Gijsen *et al.* 1999) or higher for different mucus (Li *et al.* 2008; Vélez-Cordero & Lauga 2013); dilute aqueous solutions of xanthan gum (100–1000 p.p.m.) have  $\lambda$  of the order of seconds (Gagnon *et al.* 2014). Taking  $\lambda=1$  s, we have  $Cu=\lambda\Omega=100$ , which leads to a backward propulsion velocity,  $U/a\Omega\approx-0.025$  or  $U\approx-1.65~\mu m~{\rm s}^{-1}$  (even faster than

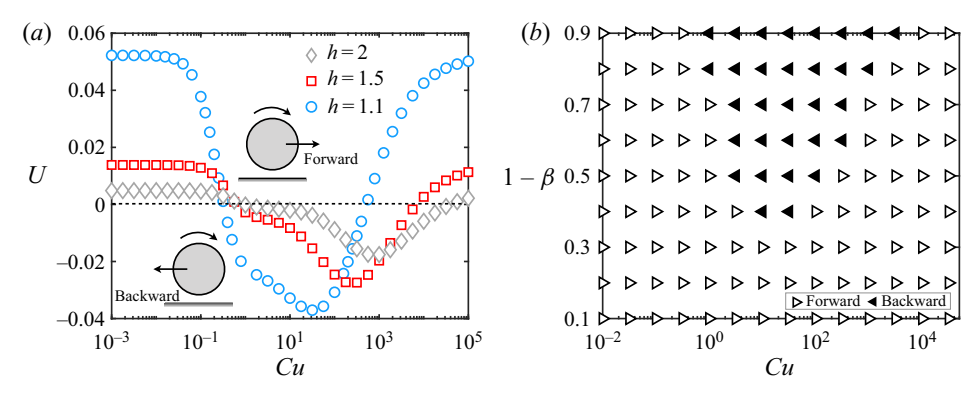


Figure 5. (a) The induced translational velocity U of a rotating sphere as a function of Cu for different distances h, when the shear-thinning effect is more substantial with a viscosity ratio  $\beta = 0.1$ . The rotating sphere can translate either forward (U > 0) or backward (U < 0) depending on the value of Cu. (b) The direction of induced translation (forward or backward) is indicated for different values of Cu and  $\beta$  for a rotating sphere at a distance h = 1.5 from the wall. Here, n = 0.25.

the Newtonian speed) from figure 5(a). We therefore expect the backward speed to be considerable and call for subsequent experimental investigations.

We also remark on the connection between the physical mechanism in the present work and those underlying the peculiar motion of a rotating sphere near a plane fluid interface in a Newtonian fluid (Lee, Chadwick & Leal 1979; Lee & Leal 1980). In the latter case, the existence of a substantial slip velocity on the fluid interface acts to reduce the velocity gradients and hence stresses on the side of the sphere closer to the interface. Such a mechanism can also cause the rotating sphere to translate in the backward mode. In this work we report a new mechanism of a distinct physical origin (non-Newtonian in nature) that can cause a similar backward translation but without requiring the presence of a fluid interface.

Finally, we suggest a potential implication of the current mechanism on the near-wall motion of swimming bacteria. Swimmer–surface interactions are known to cause clockwise circular motion of bacteria above a solid wall (Lauga *et al.* 2006) but anticlockwise motion below a free surface (Lemelle *et al.* 2010; Di Leonardo *et al.* 2011); more recently, anticlockwise motion was also observed in complex fluids and interfaces (Lemelle *et al.* 2013; Morse *et al.* 2013; Lopez & Lauga 2014). In addition, sign reversal in the self-mobilities and pair mobilities can occur for particles near elastic membranes (Daddi-Moussa-Ider *et al.* 2018*a*), which was also shown to have interesting implications on the direction of circular swimming (Daddi-Moussa-Ider *et al.* 2019).

The present work suggests another plausible mechanism that may change the direction of circular motion: the modified translation-rotation coupling due to shear-thinning rheology could, in principle, flip the direction of the wall-induced force couple on the rotating flagella and the counter-rotating cell body, thereby causing also anticlockwise circular motion even above a solid wall. Indeed, the bidirectionality of the translation-rotation coupling and its dependence on Cu as shown in figure 5 allow a bacterium (or a similar artificial microswimmer) to undergo circular motion in either direction in a shear-thinning fluid by adjusting the rotational frequency. As a remark, in addition to the direction of circular motion, the shear-thinning effect may affect the bacterial swimming speed near a wall. Subsequent studies on the detailed near-wall dynamics of swimming bacteria in a shear-thinning fluid and its connection to the

measurement of bacterial motor torque (Giacché, Ishikawa & Yamaguchi 2010; Das & Lauga 2018) could be interesting directions for future work.

### 4. Conclusion

In this work, we uncover a new physical mechanism that leads to somewhat counterintuitive behaviours of a rotating particle near a wall. In two dimensions, the shear-thinning effect causes a rotating cylinder always to translate in a direction opposite to what might be intuitively expected for an object rolling on the wall. In three dimensions, a rotating sphere may propel either forwards or backwards depending on its rotational frequency and properties of the shear-thinning fluid. Knowledge here is crucial in guiding the choice of rotational frequency of a microroller in order for it to propel effectively in the desired direction when used as a micro-propelling device. This non-Newtonian behaviour also enables more complex manoeuvres of microrollers such as bidirectional translation by simply varying the rotational frequency, without switching the direction of the external actuation field. We also discuss a potential implication of the modified translation—rotation coupling on the circular motion of swimming bacteria near a wall in complex fluids.

Taken together, we expect the present work to not only open up possibilities of more sophisticated manoeuvres of micromachines but also spur further interests in its implications on cell locomotion as well as the control of collective motion of active particles under confinement (Bricard *et al.* 2015; Driscoll *et al.* 2017) in complex fluids.

**Funding.** We acknowledge the National Science Foundation for funding support under CBET-1931292 (to O.S.P.), CBET-1931214 (to W.G.) and DMS-1951600 (to Y.-N.Y.). Y.-N.Y. also acknowledges support from Flatiron Institute, part of Simons Foundation. Computational resources from the WAVE computing facility (enabled by the E.L. Wiegand Foundation) at Santa Clara University are also gratefully acknowledged.

**Declaration of interests.** The authors report no conflict of interest.

#### Author ORCIDs.

- Ebru Demir https://orcid.org/0000-0002-2099-1679;
- Y.-N. Young https://orcid.org/0000-0001-9771-5480;
- On Shun Pak https://orcid.org/0000-0003-1510-7049.

#### REFERENCES

- AHMED, D., SUKHOV, A., HAURI, D., RODRIGUE, D., MARANTA, G., HARTING, J. & NELSON, B.J. 2021 Bioinspired acousto-magnetic microswarm robots with upstream motility. *Nat. Mach. Intell.* 3, 116–124.
- ALAPAN, Y., BOZUYUK, U., ERKOC, P., KARACAKOL, A.C. & SITTI, M. 2020 Multifunctional surface microrollers for targeted cargo delivery in physiological blood flow. *Sci. Robot.* **5** (42), eaba5726.
- BIRD, R.B., ARMSTRONG, R.C. & HASSAGER, O. 1987 Dynamics of Polymeric Liquids. 1: Fluid Mechanics. John Wiley and Sons.
- BRICARD, A., CAUSSIN, J.-B., DAS, D., SAVOIE, C., CHIKKADI, V., SHITARA, K., CHEPIZHKO, O., PERUANI, F., SAINTILLAN, D. & BARTOLO, D. 2015 Emergent vortices in populations of colloidal rollers. *Nat. Commun.* **6**, 7470.
- CHO, Y.I. & KENSEY, K.R. 1991 Effects of the non-Newtonian viscosity of blood on flows in a diseased arterial vessel. Part 1: Steady flows. *Biorheology* 28 (3–4), 241–262.
- DADDI-MOUSSA-IDER, A., KURZTHALER, C., HOELL, C., ZÖTTL, A., MIRZAKHANLOO, M., ALAM, M.-R., MENZEL, A.M., LÖWEN, H. & GEKLE, S. 2019 Frequency-dependent higher-order stokes singularities near a planar elastic boundary: implications for the hydrodynamics of an active microswimmer near an elastic interface. *Phys. Rev.* E **100**, 032610.
- DADDI-MOUSSA-IDER, A., LISICKI, M., GEKLE, S., MENZEL, A.M. & LÖWEN, H. 2018a Hydrodynamic coupling and rotational mobilities near planar elastic membranes. *J. Chem. Phys.* **149**, 014901.

- DADDI-MOUSSA-IDER, A., RALLABANDI, B., GEKLE, S. & STONE, H.A. 2018b Reciprocal theorem for the prediction of the normal force induced on a particle translating parallel to an elastic membrane. *Phys. Rev. Fluids* 3, 084101.
- DAS, D. & LAUGA, E. 2018 Computing the motor torque of escherichia coli. Soft Matt. 14, 5955-5967.
- DATT, C., ZHU, L., ELFRING, G.J. & PAK, O.S. 2015 Squirming through shear-thinning fluids. J. Fluid Mech. 784, R1.
- DEAN, W.R. & O'NEILL, M.E. 1963 A slow motion of viscous liquid caused by the rotation of a solid sphere. *Mathematika* **10** (1), 13–24.
- DEMIR, E., LORDI, N., DING, Y. & PAK, O.S. 2020 Nonlocal shear-thinning effects substantially enhance helical propulsion. *Phys. Rev. Fluids* 5, 111301.
- DI LEONARDO, R., DELL'ARCIPRETE, D., ANGELANI, L. & IEBBA, V. 2011 Swimming with an image. *Phys. Rev. Lett.* **106**, 038101.
- DRISCOLL, M., DELMOTTE, B., YOUSSEF, M., SACANNA, S., DONEV, A. & CHAIKIN, P. 2017 Unstable fronts and motile structures formed by microrollers. *Nat. Phys.* 13, 375–379.
- ELFRING, G.J. 2017 Force moments of an active particle in a complex fluid. J. Fluid Mech. 829, R3.
- ELFRING, G.J. & LAUGA, E. 2015 Theory of locomotion through complex fluids. In *Complex Fluids in Biological Systems* (ed. S.E. Spagnolie), pp. 283–317. Springer.
- ELGETI, J. & GOMPPER, G. 2016 Microswimmers near surfaces. Eur. Phys. J. 225, 2333-2352.
- FANG, W.-Z., HAM, S., QIAO, R. & TAO, W.-Q. 2020 Magnetic actuation of surface walkers: the effects of confinement and inertia. *Langmuir* 36 (25), 7046–7055.
- GAGNON, D.A. & ARRATIA, P.E. 2016 The cost of swimming in generalized Newtonian fluids: experiments with *C. elegans. J. Fluid Mech.* **800**, 753–765.
- GAGNON, D.A., KEIM, N.C. & ARRATIA, P.E. 2014 Undulatory swimming in shear-thinning fluids: experiments with *Caenorhabditis elegans*. *J. Fluid Mech.* **758**, R3.
- GIACCHÉ, D., ISHIKAWA, T. & YAMAGUCHI, T. 2010 Hydrodynamic entrapment of bacteria swimming near a solid surface. *Phys. Rev.* E **82**, 056309.
- GIJSEN, F.J.H., VAN DE VOSSE, F.N. & JANSSEN, J.D. 1999 The influence of the non-Newtonian properties of blood on the flow in large arteries: steady flow in a carotid bifurcation model. *J. Biomech.* **32** (6), 601–608.
- GÓMEZ, S., GODÍNEZ, F.A., LAUGA, E. & ZENIT, R. 2017 Helical propulsion in shear-thinning fluids. J. Fluid Mech. 812, R3.
- HAN, K., SHIELDS IV, C.W., BHARTI, B., ARRATIA, P.E. & VELEV, O.D. 2020 Active reversible swimming of magnetically assembled 'microscallops' in non-Newtonian fluids. *Langmuir* **36** (25), 7148–7154.
- JEFFREY, D.J. & ONISHI, Y. 1981 The slow motion of a cylinder next to a plane wall. *Q. J. Mech. Appl. Maths* **34** (2), 129–137.
- LAUGA, E. 2014 Locomotion in complex fluids: integral theorems. Phys. Fluids 26 (8), 081902.
- LAUGA, E., DILUZIO, W.R., WHITESIDES, G.M. & STONE, H.A. 2006 Swimming in circles: motion of bacteria near solid boundaries. *Biophys. J.* **90**, 400–412.
- LEAL, L.G. 1980 Particle motions in a viscous fluid. Annu. Rev. Fluid Mech. 12 (1), 435-476.
- LEE, S.H., CHADWICK, R.S. & LEAL, L.G. 1979 Motion of a sphere in the presence of a plane interface. Part 1. An approximate solution by generalization of the method of Lorentz. *J. Fluid Mech.* 93 (4), 705–726.
- LEE, S.H. & LEAL, L.G. 1980 Motion of a sphere in the presence of a plane interface. Part 2. An exact solution in bipolar co-ordinates. *J. Fluid Mech.* **98** (1), 193–224.
- LEMELLE, L., PALIERNE, J.-F., CHATRE, E. & PLACE, C. 2010 Counterclockwise circular motion of bacteria swimming at the air-liquid interface. *J. Bacteriol.* **192**, 6307–6308.
- LEMELLE, L., PALIERNE, J.-F., CHATRE, E., VAILLANT, C. & PLACE, C. 2013 Curvature reversal of the circular motion of swimming bacteria probes for slip at solid/liquid interfaces. *Soft Matt.* **9**, 9759–9762.
- LI, G. & ARDEKANI, A.M. 2015 Undulatory swimming in non-Newtonian fluids. J. Fluid Mech. 784, R4.
- LI, W.G., LUO, X.Y., CHIN, S.B., HILL, N.A., JOHNSON, A.G. & BIRD, N.C. 2008 Non-Newtonian bile flow in elastic cystic duct: one- and three-dimensional modeling. *Ann. Biomed. Engng* **36**, 1893–1908.
- LOPEZ, D. & LAUGA, E. 2014 Dynamics of swimming bacteria at complex interfaces. *Phys. Fluids* **26** (7), 071902.
- MASOUD, H. & STONE, H.A. 2019 The reciprocal theorem in fluid dynamics and transport phenomena. J. Fluid Mech. 879, P1.
- MONTENEGRO-JOHNSON, T.D. 2017 Fake μs: a cautionary tail of shear-thinning locomotion. *Phys. Rev. Fluids* **2**, 081101.
- MONTENEGRO-JOHNSON, T.D., SMITH, D.J. & LOGHIN, D. 2013 Physics of rheologically enhanced propulsion: different strokes in generalized stokes. *Phys. Fluids* **25**, 081903.

- MORSE, M., HUANG, A., LI, G., MAXEY, M.R. & TANG, J.X. 2013 Molecular adsorption steers bacterial swimming at the air/water interface. *Biophys. J.* **105**, 21–28.
- O'NEILL, M.E. 1964 A slow motion of viscous liquid caused by a slowly moving solid sphere. *Mathematika* 11 (1), 67–74.
- O'NEILL, M.E. 1967 A slow motion of viscous liquid caused by a slowly moving solid sphere: an addendum. *Mathematika* **14** (2), 170–172.
- PARK, J.-S., KIM, D., SHIN, J.H. & WEITZ, D.A. 2016 Efficient nematode swimming in a shear thinning colloidal suspension. *Soft Matt.* 12, 1892–1897.
- QIU, T., LEE, T.-C., MARK, A.G., MOROZOV, K.I., MÜNSTER, R., MIERKA, O., TUREK, S., LESHANSKY, A.M. & FISCHER, P. 2014 Swimming by reciprocal motion at low Reynolds number. *Nat. Commun.* 5, 5119.
- QU, Z. & Breuer, K.S. 2020 Effects of shear-thinning viscosity and viscoelastic stresses on flagellated bacteria motility. Phys. Rev. Fluids 5, 073103.
- SING, C.E., SCHMID, L., SCHNEIDER, M.F., FRANKE, T. & ALEXANDER-KATZ, A. 2010 Controlled surface-induced flows from the motion of self-assembled colloidal walkers. *Proc. Natl Acad. Sci. USA* **107** (2), 535–540.
- SPAGNOLIE, S.E. & LAUGA, E. 2012 Hydrodynamics of self-propulsion near a boundary: predictions and accuracy of far-field approximations. *J. Fluid Mech.* **700**, 105–147.
- SZNITMAN, J. & ARRATIA, P.E. 2015 Locomotion through complex fluids: an experimental view. In *Complex Fluids in Biological Systems* (ed. S.E. Spagnolie), pp. 245–281. Springer.
- TAKAGI, D., PALACCI, J., BRAUNSCHWEIG, A.B., SHELLEY, M.J. & ZHANG, J. 2014 Hydrodynamic capture of microswimmers into sphere-bound orbits. *Soft Matt.* 10, 1784–1789.
- TIERNO, P., GOLESTANIAN, R., PAGONABARRAGA, I. & SAGUÉS, F. 2008 Controlled swimming in confined fluids of magnetically actuated colloidal rotors. *Phys. Rev. Lett.* **101**, 218304.
- VÉLEZ-CORDERO, J.R. & LAUGA, E. 2013 Waving transport and propulsion in a generalized Newtonian fluid. *J. Non-Newtonian Fluid Mech.* **199**, 37–50.
- WANG, J. & JOSEPH, D.D. 2003 Lift forces on a cylindrical particle in plane Poiseuille flow of shear thinning fluids. *Phys. Fluids* **15** (8), 2267–2278.